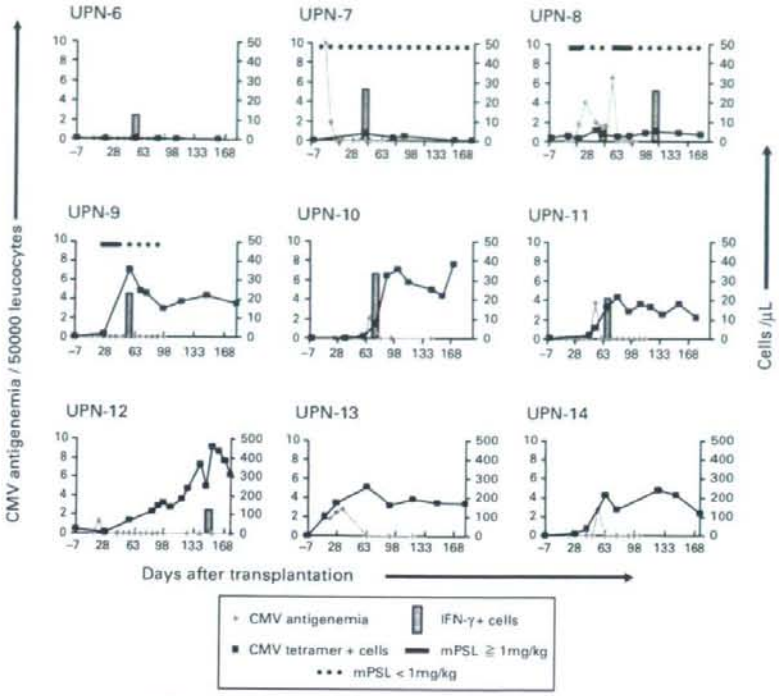

Figure 3 Serial analysis in patients with CMV antigenemia of $<10/50\,000$ or patients without CMV antigenemia. The legends are the same as Figure 2. Intracellular cytokine was not assessed for UPN13 and UPN14.

Table 1 Patients' characteristics

ID	*Age*	*HLA-A locus*	*Primary disease*	*Conditioning regimen*	*GVHD prophylaxis*	*Stem cell source*	*CMV serology*		*Max CMV-Ag*	*CMV disease*
							Recipient	*Donor*		
UPN-01	63	0201, 0206	CML (AP)	CdA/BU	CSP→TAC	PB	+	+	740	+
UPN-02	57	0201	NHL (DLBCL)	CdA/BU	CSP	PB	+	+	48	+
UPN-03	49	0201	NHL (low grade)	CdA/BU	CSP→TAC	PB	+	+	178	+
UPN-04	54	0206	MCL	CdA/BU/ ATG	CSP + sMTX	PB	+	+	68	–
UPN-05	59	0206	AML	CdA/BU/TBI	CSP + sMTX	UBM	+	+	35	–
UPN-06	66	0206	MDS (RA)	Flu/BU	CSP + sMTX	PB	+	–	0	–
UPN-07	61	0201	NHL (low grade)	Flu/BU/ATG	CSP	UBM	+	+	10	–
UPN-08	62	0201	AML	CdA/BU	TAC	PB	+	+	6.5	–
UPN-09	43	0201	MDS (RA)	BU/CY	CSP + sMTX	UBM	+	–	0	–
UPN-10	41	0206	AML	BU/CY	CSP + sMTX	RBM	+	+	2.1	–
UPN-11	54	0201	NHL (low grade)	Flu/BU	CSP + sMTX	PB	+	+	3.7	–
UPN-12	32	0206	RCC	CdA/BU	CSP	PB	+	+	2.8	–
UPN-13	42	0206	PCL	CdA/BU/ ATG	CSP + sMTX	PB	+	+	2.8	–
UPN-14	43	0206	RCC	CdA/BU/ ATG	CSP	PB	+	+	1.3	–

Abbreviations: ATG = antithymocyte globulin; CdA = cladribine; CML (AP) = CML (accelerated phase); CSP = cyclosporine; DLBCL = diffuse large B-cell lymphoma; Flu = fludarabine; MCL = mantle cell lymphoma; MDS (RA) = myelodysplastic syndrome (refractory anemia); NHL = non-Hodgkin lymphoma; PB = peripheral blood; PCL = plasma cell leukemia; RBM = related bone marrow; RCC = renal cell carcinoma; sMTX = short term methotrexate; TAC = tacrolimus; UBM = unrelated bone marrow.

antigenemia and required antiviral therapy showed that the mean number of IFN-γ-producing cells was 3.6 (0–6.7)/μl at day 60, which subsequently increased to 72 (15–250)/μl at day 160. As for three patients with CMV colitis (UPN1–3), only one patient (UPN2) had detectable level of IFN-γ-producing cells (4.8/μl) at the time of disease

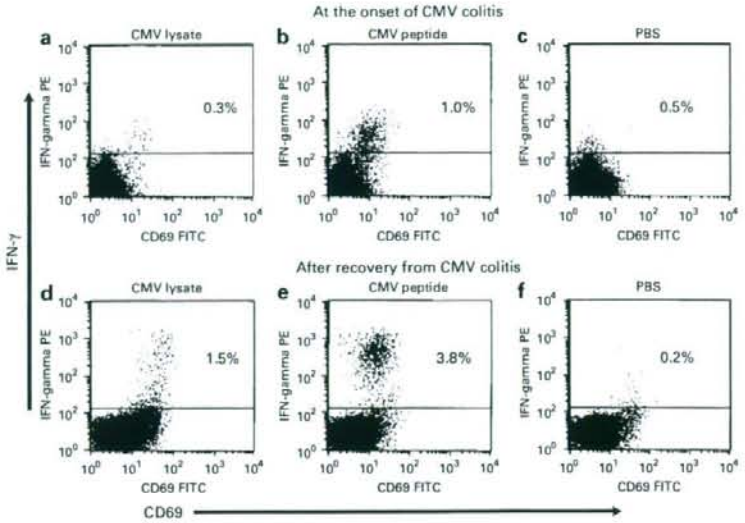

Figure 4 Intracellular cytokine assay in a patient with CMV colitis (UPN2). The samples were taken at the onset of CMV colitis (**a**–**c**) and after recovery from CMV colitis (**d**–**f**). The numbers of IFN-γ-producing cells on lysate stimulation (**a**, **d**) and peptide stimulation (**b**, **e**) both increased after recovery from CMV colitis. (**c**) and (**f**) are negative controls.

onset and were undetectable for the other two patients, which remained negative until day 90 for UPN1. The mean number of IFN-γ+ cells subsequently increased to 19 (5–38)/μl after recovery from CMV disease (Figures 2, 4a and d). Among the patients who did not require antiviral therapy, the IFN-γ-producing cells were all >10/μl at day 60.

When stimulated with CMV peptide, IFN-γ-producing cells numbered 8 (0–16)/μl at the time of disease onset with a subsequent increase to 47 (15–95)/μl after recovery from CMV disease (Figures 4b and e).

Regarding the phenotype of IFN-γ-producing cells, median of 81% (76–100) were CD4+ and <20% were CD8+ upon stimulation by CMV lysate. The staining of IFN-γ was brighter in CD4+ than in CD8+ cells and CD69 was positive for both CD4+ and CD8+ fraction. IFN-γ-producing cells were CD69 low positive and median of 42% (25–68) were CD8+, while the rest were CD8−/CD4− phenotype upon CMV peptide stimulation.

Discussion

Our results showed that it is difficult to predict CMV infection by the number of CMV-specific CTL alone as this did not correlate with the incidence and severity of CMV infection. While UPN1 and UPN2 developed CMV colitis after the recovery of sufficient number of CTL, UPN6, UPN7 and UPN8 did not require antiviral therapy despite low CMV-specific CTL. These results showed that CMV disease could occur after HSCT even in patients with >10/μl CMV-specific CTL as evaluated by tetramer assay, which has been considered to be sufficient to protect against CMV infection.[5,7]

CMV-specific CTL emerged immediately following the detection of antigenemia in most patients, suggesting that CMV infection can be a trigger for the recovery of CMV-specific immunity. However, UPN9 had recovery of CMV-specific CTL at day 60 even though his CMV antigenemia and CMV DNA as evaluated by PCR were negative throughout the course.

On the other hand, intracellular analysis revealed that IFN-γ production in both CD4+ and CD8+ T lymphocytes was depressed in patients with high antigenemia or CMV disease and this had subsequently recovered at disease resolution. Functional analysis methods for CMV-specific immune response by flow cytometry have been established,[16] and it was reported that patients who developed CMV disease after SCT had no detectable IFN-γ production by CD3+/4+ T-cells upon CMV AD-169 antigen stimulation.[17] It has also been demonstrated that levels of IFN-γ-producing CD4+ cells less than one cell/μl and CD8+ less than three cells/μl upon stimulation by CMV-infected autologous dendritic cells are not protective against recurrent infection.[18] As assessed by IFN-γ ELISPOT assay, the threshold level for protection against CMV reactivation was estimated as over one cell/μl peripheral blood upon CMV pp65 peptide stimulation.[19] The number of IFN-γ-producing cells upon CMV lysate stimulation were above ten cells/μl among patients whose antigenemia was <10/50 000 cells in our study, which may be sufficient for protection against CMV reactivation. It is difficult to determine the exact threshold level for protection against CMV since IFN-γ production differs among various stimulating agents. Also the magnitude of response is higher in the cytokine flow cytometry assay while the cytokine flow cytometry assay was less likely than the ELISPOT assay to detect low-level responses.[20]

Several studies on HIV-infected patients have shown the availability of analyzing the phenotype and other cytokine production of virus-specific T-cells such as IL-2, TNF-α.[21–23] It has been demonstrated that virus-specific T-cells, which produce both IFN-γ and IL-2 are important in virus-specific immunity, and that IFN-γ/IL-2 secreting CD8+ T-cells were CD45RA−/CCR7− phenotype and correlated with that of proliferating T-cells, whereas single IFN-γ-secreting cells were either CD45RA−/CCR7− or CD45RA+/CCR7−.[22] Another study has shown that immunorestored patients had increased levels of circulating CMV-specific CD8+ T-cells with 'early' (CD27+/CD28+/CD45RA+, CD27+/CD28+/CD45RA−) and 'intermediate' (CD27−/CD28+/CD45RA−) phenotype.[23] Only IFN-γ production was assessed in our study, however higher-order flow cytometry might have added more discriminatory value. Foster *et al*.[24] demonstrated that CMV-specific CD4+ T-helper cells show the same reconstitution kinetics as CD8+ CTL. Thus, functional analysis of lymphocytes upon lysate stimulation that can be used to assess both CD4+ and CD8+ cells is a useful tool for monitoring T cell immunity against CMV in patients after HSCT. This method is more widely applicable than peptide stimulation or tetramer assay, since it is not restricted to HLA or a single epitope. However, peptide stimulation and tetramer assay may still be a major procedure in the analysis of CD8+ T-cells, since tetramers are widely applied to adoptive immunotherapy of CMV[25] and the dominant population of IFN-γ-producing cells upon lysate stimulation was CD4+. Previous study has demonstrated that flow cytometry following stimulation of PBMC with pp65 and immediate early (IE)-1 peptide pools consisted of 15-aa peptides was highly sensitive and specific in predicting the presence of recognized epitope in the respective proteins.[26] Furthermore, it has been shown that IE-1-specific responses were more important in protective immunity than pp65-specific responses in heart and lung transplant recipients.[27] The stimulation with comprehensive peptide pools might have better assessed both functional CD4+ and CD8+ T-cell responses. Further study is needed to identify whether IE-1 is more important than pp65 in allogeneic HSCT patients, and the significance of IE-1 in Japanese population with low allele frequency of HLA-A1 (1.8%), -B7 (5.2%) or -B8 (< 1%),[15] which is known to present IE-1 epitopes.

It is likely that the patients who did not have CMV reactivation despite low CMV-specific CTL had sufficient T-cell immune-recovery against CMV since the number of intracellular IFN-γ positive cells upon CMV lysate stimulation was as high as that in patients who had recovered from CMV reactivation. As for CD8+ T cells in these patients, CTL against other CMV-epitopes besides NLV might have helped to protect against CMV. It is reported that the recovery of CMV specific T-cells is earlier in patients who received reduced-intensity conditioning compared to conventional regimen and this was delayed by the use of ATG.[19,28] Additionally, the graft source and CD3+ T-cell dose significantly influence the recovery of CMV-specific immunity.[28] The difference of immune recovery according to the conditioning regimen and graft source was not demonstrated in this study, probably due to heterogeneous patients and small sample size. Functional depression of the lymphocytes due to corticosteroid for GVHD seems to be the major cause of CMV infection as documented in all patients with high antigenemia. Moreover, 75% of the patients with CMV disease were receiving more than 1 mg/kg/day of methylprednisolone (mPSL), while among those who did not require antiviral therapy, only 13% had received 1 mg/kg/day or more mPSL. The influence of corticosteroid on the number of CMV-specific CTL is controversial. Some studies have reported that a significant reduction of CMV-specific CTL occurred with corticosteroid therapy.[6,8] Others have shown that the frequency and the absolute number of CMV-specific CD8+ T cells were similar in patients receiving corticosteroids and those who didn't, while the CMV-specific CD8+ T cells showed decreased cytokine production.[10,11] Our result was consistent with the latter observation that while the number of CMV-specific CTL does not decrease significantly with corticosteroid therapy, IFN-γ production of CMV-specific CTL is severely suppressed. Therefore, concomitant assessment of T-cell function is essential in patients after HSCT, especially in those who are receiving corticosteroid therapy.

References

1 Boeckh M, Nichols WG, Papanicolaou G, Rubin R, Wingard JR, Zaia J. Cytomegalovirus in hematopoietic stem cell transplant recipients: current status, known challenges, and future strategies. *Biol Blood Marrow Transplant* 2003; **9**: 543–558.

2 Zaia JA, Sissons JG, Riddell S, Diamond DJ, Wills MR, Carmichael AJ *et al*. Status of Cytomegalovirus Prevention and Treatment in 2000. *Hematology (Am Soc Hematol Educ Program)* 2000, 339–355.

3 Lacey SF, Villacres MC, La Rosa C, Wang Z, Longmate J, Martinez J *et al*. Relative dominance of HLA-B*07 restricted CD8+ T-lymphocyte immune responses to human cytomegalovirus pp65 in persons sharing HLA-A*02 and HLA-B*07 alleles. *Hum Immunol* 2003; **64**: 440–452.

4 Singhal S, Shaw JC, Ainsworth J, Hathaway M, Gillespie GM, Paris H *et al*. Direct visualization and quantitation of cytomegalovirus-specific CD8+ cytotoxic T-lymphocytes in liver transplant patients. *Transplantation* 2000; **69**: 2251–2259.

5 Gratama JW, van Esser JW, Lamers CH, Tournay C, Lowenberg B, Bolhuis RL *et al*. Tetramer-based quantification of cytomegalovirus (CMV)-specific CD8+ T lymphocytes in T-cell-depleted stem cell grafts and after transplantation may identify patients at risk for progressive CMV infection. *Blood* 2001; **98**: 1358–1364.

6 Aubert G, Hassan-Walker AF, Madrigal JA, Emery VC, Morte C, Grace S *et al*. Cytomegalovirus-specific cellular immune responses and viremia in recipients of allogeneic stem cell transplants. *J Infect Dis* 2001; **184**: 955–963.

7 Cwynarski K, Ainsworth J, Cobbold M, Wagner S, Mahendra P, Apperley J *et al*. Direct visualization of cytomegalovirus-specific T-cell reconstitution after allogeneic stem cell transplantation. *Blood* 2001; **97**: 1232–1240.

8 Engstrand M, Tournay C, Peyrat MA, Eriksson BM, Wadstrom J, Wirgart BZ *et al*. Characterization of CMVpp65-specific CD8+ T lymphocytes using MHC tetramers in kidney transplant patients and healthy participants. *Transplantation* 2000; **69**: 2243–2250.

9 Lacey SF, Gallez-Hawkins G, Crooks M, Martinez J, Senitzer D, Forman SJ *et al*. Characterization of cytotoxic function of CMV-pp65-specific CD8+ T-lymphocytes identified by HLA tetramers in recipients and donors of stem-cell transplants. *Transplantation* 2002; **74**: 722–732.

10 Engstrand M, Lidehall AK, Totterman TH, Herrman B, Eriksson BM, Korsgren O. Cellular responses to cytomegalovirus in immunosuppressed patients: circulating CD8+ T cells recognizing CMVpp65 are present but display functional impairment. *Clin Exp Immunol* 2003; **132**: 96–104.

11 Ozdemir E, St John LS, Gillespie G, Rowland-Jones S, Champlin RE, Molldrem JJ *et al*. Cytomegalovirus reactivation following allogeneic stem cell transplantation is associated with the presence of dysfunctional antigen-specific CD8+ T cells. *Blood* 2002; **100**: 3690–3697.

12 Morita Y, Hosokawa M, Ebisawa M, Sugita T, Miura O, Takaue Y *et al*. Evaluation of cytomegalovirus-specific cytotoxic T-lymphocytes in patients with the HLA-A*02 or HLA-A*24 phenotype undergoing hematopoietic stem cell transplantation. *Bone Marrow Transplant* 2005; **36**: 803–811.

13 Morita Y, Heike Y, Kawakami M, Miura O, Nakatsuka S, Ebisawa M *et al*. Monitoring of WT1-specific cytotoxic T lymphocytes after allogeneic hematopoietic stem cell transplantation. *Int J Cancer* 2006; **119**: 1360–1367.

14 Rauser G, Einsele H, Sinzger C, Wernet D, Kuntz G, Assenmacher M *et al*. Rapid generation of combined CMV-specific CD4+ and CD8+ T-cell lines for adoptive transfer into recipients of allogeneic stem cell transplants. *Blood* 2004; **103**: 3565–3572.

15 Tokunaga K, Ishikawa Y, Ogawa A, Wang H, Mitsunaga S, Moriyama S *et al*. Sequence-based association analysis of HLA class I and II alleles in Japanese supports conservation of common haplotypes. *Immunogenetics* 1997; **46**: 199–205.

16 Waldrop SL, Pitcher CJ, Peterson DM, Maino VC, Picker LJ. Determination of antigen-specific memory/effector CD4+ T cell frequencies by flow cytometry: evidence for a novel, antigen-specific homeostatic mechanism in HIV-associated immunodeficiency. *J Clin Invest* 1997; **99**: 1739–1750.

17 Avetisyan G, Larsson K, Aschan J, Nilsson C, Hassan M, Ljungman P. Impact on the cytomegalovirus (CMV) viral load by CMV-specific T-cell immunity in recipients of allogeneic stem cell transplantation. *Bone Marrow Transplant* 2006; **38**: 687–692.

18 Lilleri D, Gerna G, Fornara C, Lozza L, Maccario R, Locatelli F. Prospective simultaneous quantification of human cytomegalovirus-specific CD4+ and CD8+ T-cell reconstitution in young recipients of allogeneic hematopoietic stem cell transplants. *Blood* 2006; **108**: 1406–1412.

19 Ohnishi M, Sakurai T, Heike Y, Yamazaki R, Kanda Y, Takaue Y *et al*. Evaluation of cytomegalovirus-specific T-cell reconstitution in patients after various allogeneic haematopoietic stem cell transplantation using interferon-gamma-enzyme-linked immunospot and human leucocyte antigen tetramer assays with an immunodominant T-cell epitope. *Br J Haematol* 2005; **131**: 472–479.

20 Karlsson AC, Martin JN, Younger SR, Bredt BM, Epling L, Ronquillo R *et al*. Comparison of the ELISPOT and cytokine flow cytometry assays for the enumeration of antigen-specific T cells. *J Immunol Methods* 2003; **283**: 141–153.

21 Betts MR, Nason MC, West SM, De Rosa SC, Migueles SA, Abraham J *et al*. HIV nonprogressors preferentially maintain highly functional HIV-specific CD8+ T cells. *Blood* 2006; **107**: 4781–4789.

22 Zimmerli SC, Harari A, Cellerai C, Vallelian F, Bart PA, Pantaleo G. HIV-1-specific IFN-gamma/IL-2-secreting CD8 T cells support CD4-independent proliferation of HIV-1-specific CD8 T cells. *Proc Natl Acad Sci USA* 2005; **102**: 7239–7244.

23 Sinclair E, Tan QX, Sharp M, Girling V, Poon C, Natta MV *et al*. Protective immunity to cytomegalovirus (CMV) retinitis in AIDS is associated with CMV-specific T cells that express interferon- gamma and interleukin-2 and have a CD8+ cell early maturational phenotype. *J Infect Dis* 2006; **194**: 1537–1546.

24 Foster AE, Gottlieb DJ, Sartor M, Hertzberg MS, Bradstock KF. Cytomegalovirus-specific CD4+ and CD8+ T-cells follow a similar reconstitution pattern after allogeneic stem cell transplantation. *Biol Blood Marrow Transplant* 2002; **8**: 501–511.

25 Cobbold M, Khan N, Pourgheysari B, Tauro S, McDonald D, Osman H *et al*. Adoptive transfer of cytomegalovirus-specific CTL to stem cell transplant patients after selection by HLA-peptide tetramers. *J Exp Med* 2005; **202**: 379–386.

26 Kern F, Faulhaber N, Frommel C, Khatamzas E, Prosch S, Schonemann C *et al*. Analysis of CD8 T cell reactivity to cytomegalovirus using protein-spanning pools of overlapping pentadecapeptides. *Eur J Immunol* 2000; **30**: 1676–1682.

27 Bunde T, Kirchner A, Hoffmeister B, Habedank D, Hetzer R, Cherepnev G *et al*. Protection from cytomegalovirus after transplantation is correlated with immediate early 1-specific CD8 T cells. *J Exp Med* 2005; **201**: 1031–1036.

28 Mohty M, Mohty AM, Blaise D, Faucher C, Bilger K, Isnardon D *et al*. Cytomegalovirus-specific immune recovery following allogeneic HLA-identical sibling transplantation with reduced-intensity preparative regimen. *Bone Marrow Transplant* 2004; **33**: 839–846.

References

1. van Ommen CH, Peters M. Venous thromboembolic disease in childhood. Semin Thromb Hemost 2003;29:391–404.
2. Wells PS, Anderson DR, Rodger M, et al. Evaluation of D-dimer in the diagnosis of suspected deep-vein thrombosis. N Engl J Med 2003;349:1227–1235.
3. 510(k) Summary for Advanced D-dimer Assay. Rockville, MD: Office of In Vitro Diagnostic Devices: Food and Drug Administration; 2004.
4. Brotman DJ, Segal JB, Jani JT, et al. Limitations of D-dimer testing in unselected inpatients with suspected venous thromboembolism. Am J Med 2003;114:276–282.
5. Rajpurkar M, Warrier I, Chitlur M, et al. Pulmonary embolism–experience at a single children's hospital. Thromb Res 2007;119:699–703.
6. Goldenberg NA, Knapp-Clevenger R, Manco-Johnson MJ. Elevated plasma factor VIII and D-dimer levels as predictors of poor outcomes of thrombosis in children. N Engl J Med 2004;351:1081–1088.
7. Eichinger S, Minar E, Bialonczyk C, et al. D-dimer levels and risk of recurrent venous thromboembolism. JAMA 2003;290:1071–1074.
8. Palareti G, Legnani C, Cosmi B, et al. Predictive value of D-dimer test for recurrent venous thromboembolism after anticoagulation withdrawal in subjects with a previous idiopathic event and in carriers of congenital thrombophilia. Circulation 2003;108:313–318.
9. Lensing AW, Prandoni P, Brandjes D, et al. Detection of deep-vein thrombosis by real-time B-mode ultrasonography. N Engl J Med 1989;320:342–345.
10. Sampson F, Goodacre S, Thomas S, et al. The accuracy of MRI in diagnosis of suspected deep vein thrombosis: systematic review and meta-analysis. Eur Radiol 2007;17:175–181.

Positive impact of maintaining minimal caloric intake above 1.0 × basal energy expenditure on the nutritional status of patients undergoing allogeneic hematopoietic stem cell transplantation

To the Editor: Parenteral nutrition (PN) is frequently required for patients undergoing allogeneic hematopoietic stem cell transplantation (ASCT). However, the recommended dose of PN is associated with hyperglycemia [1,2], which leads to an inferior outcome [1,3]. Body weight (BW) and biochemical indices are used to assess the nutritional status, but these measures are affected by fluid status and inflammation [4]. Therefore, we retrospectively analyzed the values of nutritional variables in a cohort of 112 consecutive adult patients, who received myeloablative ASCT between January 2002 and June 2006. Sixteen patients who died before day 28, developed renal failure or liver failure, or received previous ASCT were excluded. Based on the mean caloric intake from the beginning of the conditioning regimen to day 28 or discharge, the remaining 96 patients were divided into low (n = 67) and high (n = 29) caloric groups [< or ≥ than 1.0 × basal energy expenditure (BEE)]. Patients' characteristics are summarized in Table I. During this period, nutritional support had been left entirely to the individual physicians. Six time periods were considered: (1) before the conditioning regimen, (2) from conditioning to day 0, (3) from days 1 to 7, (4) from days 8 to 14, (5) from days 15 to 21, (6) from days 22 to 28. Biochemical indices including total protein, albumin, cholinesterase, and prealbumin were monitored serially at least once a week.

TABLE I. Patients' Characteristics

Variable	N (%)/ median (range)	
	Low caloric group < 1.0 × BEE n = 67	High caloric group ≥1.0 × BEE n = 29
Age (year)	33 (18–57)	47 (20–55)
Body mass index (kg/m²)	22.3 (15.2–38.1)	21.0 (15.1–27.2)
Sex		
Male	29 (43)	15 (52)
Female	38 (57)	14 (48)
Conditioning		
TBI-containing	34 (51)	15 (52)
Non-TBI-containing	33 (49)	14 (48)
Stem cell source		
Bone marrow	38 (57)	13 (45)
PBSC	28 (42)	12 (41)
Cord blood	1 (1)	4 (14)

Abbreviations: BEE, basal energy expenditure; TBI, total body irradiation; PBSC, peripheral blood stem cells.

Changes in BW are shown in Fig. 1A: a greater number of patients in the low caloric group lost more than 5% or 10% of their BW compared with the high caloric group (38 vs. 4, $P < 0.001$ and 8 vs 0, $P = 0.1$, respectively). No significant differences were seen for serum albumin, total proteins, cholinesterase, and prealbumin, whereas fasting glucose levels were significantly reduced from days 15 to 28 in the low caloric group (Fig. 1B). The significantly greater weight loss in the low caloric group could be associated with protein loss and organ dysfunction, although changes in fluid status and effects of chronic inflammation should also be considered. The absence of significant differences in biochemical indices between the two groups suggests that these parameters do not directly reflect malnutrition in ASCT patients [5]. Hyperglycemia was observed in patients receiving ≥1.0 × BEE caloric intake. We previously reported that hyperglycemia and neutropenia were associated with an inferior outcome [3]. The results suggest that a minimal caloric intake of >1.0 × BEE is necessary to maintain BW after ASCT, and that the assessment of nutritional status should not rely solely on biochemical indices. However, attention should be paid to the identification and prevention of hyperglycemia in these patients.

Shigeo Fuji[1]
Sung-Won Kim[1]
Takahiro Fukuda[1]
Shigemi Kamiya[2]
Setsuko Kuwahara[2]
Yoichi Takaue[1]

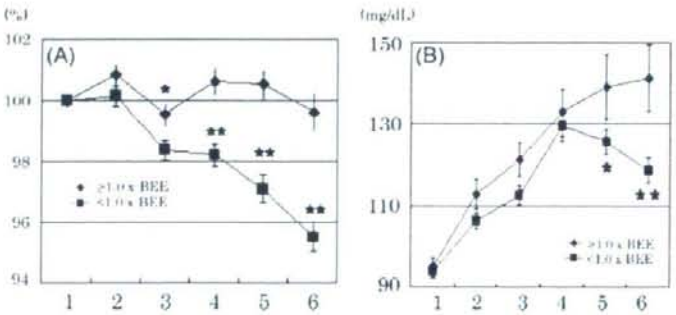

Figure 1. (A) Change in body weight in ASCT (*P 0.05, **P < 0.001). (B) Change in fasting serum glucose level in ASCT (*P 0.06, **P 0.003). The time course was divided into six periods: (1) before the conditioning regimen, (2) from conditioning to day 0, (3) from days 1 to 7, (4) from days 8 to 14, (5) from days 15 to 21, (6) from days 22 to 28.

[1]Department of Hematology and Stem Cell Transplantation, National Cancer Center Hospital, Tokyo, Japan
[2]Division of Nutritional Management, National Cancer Center Hospital, Tokyo, Japan
Published online 8 October 2008 in Wiley InterScience (www.interscience.wiley.com).
DOI: 10.1002/ajh.21307

References

1. Sheean PM, Freels SA, Helton WS, et al. Adverse clinical consequences of hyperglycemia from total parenteral nutrition exposure during hematopoietic stem cell transplantation. Biol Blood Marrow Transplant 2006;12:656–664.
2. Sheean PM, Braunschweig C, Rich E. The incidence of hyperglycemia in hematopoietic stem cell transplant recipients receiving total parenteral nutrition: A pilot study. J Am Diet Assoc 2004;104:1352–1360.
3. Fuji S, Kim SW, Mori S, et al. Hyperglycemia during the neutropenic period is associated with a poor outcome in patients undergoing myeloablative allogeneic hematopoietic stem cell transplantation. Transplantation 2007;84:814–820.
4. Kubrak C, Jensen L. Malnutrition in acute care patients: A narrative review. Int J Nurs Stud 2007;44:1036–1054.
5. Muscaritoli M, Conversano L, Cangiano C, et al. Biochemical indices may not accurately reflect changes in nutritional status after allogeneic bone marrow transplantation. Nutrition 1995;11:433–436.

IGF-I treatment of patients with Laron syndrome suppresses serum thrombopoietin levels but does not affect serum erythropoietin

To the Editor: Growth hormone (GH) and insulin-like growth factor I (IGF-I) stimulate the proliferation and differentiation of many cell types including bone marrow cells. IGF-I was shown to stimulate erythropoiesis in in vitro studies [1]. In a previous study, we reported that children with Laron syndrome (LS, OMIM #262500) with congenital IGF-I deficiency responded to IGF-I treatment by an increase of hemoglobin (Hb) and red blood cells (RBC) and a decrease of a high platelet count (PLT) [2]. To investigate whether the effects induced by IGF-I are mediated by erythropoietin (Epo) and thrombopoietin (Tpo), we studied seven patients with LS: three untreated adults (ages: 43, 44, and 52) and four girls aged: 5, 9, 13, and 15 years receiving IGF-I replacement therapy (120–180 μg/kg/day s.c., Fujisawa, Osaka, Japan) for an average period of 9 ± 4 years. The mean age at initiation of therapy was 4.6 ± 3.5 years. Serum Tpo and Epo levels were measured using ELISA kits (Quantikine, R&D Systems, Minneapolis). In the children, before initiation of IGF-I treatment, Tpo levels were above normal for age, m ± SD: 285 ± 189 pg/ml (normal: 15–80 pg/ml). During IGF-I treatment Tpo levels dropped to 36 ± 19 pg/ml ($P = 0.04$). The mean PLT levels before treatment were 334 ± 53 × 10^9/l and decreased to 253 ± 30 × 10^9/l during therapy ($P = 0.04$). In the three untreated adult patients, Tpo serum levels were above normal but the PLT were within the normal limits (Table I). In the IGF-I treated-children, Epo levels did not correlate with the increase of RBC and Hb; and in the untreated adults, Epo levels varied within normal limits (1.0–21.5 mIU/ml). Experimental studies have indicated that the effects of GH on erythropoiesis are mediated by IGF-I of endocrine or paracrine origin [3]. We report for the first time that IGF-I administration reduces the high PLT count in young LS patients concomitantly with serum Tpo levels.

TABLE I. The Effect of IGF-I on Tpo and Platelets

	Before treatment	During treatment	*P* value
LS children			
Tpo (pg/ml)	285 ± 189	36 ± 19	0.04
Platelets (×10^9/l)	334 ± 53	253 ± 30	0.04
Untreated LS adults			
Tpo (pg/ml)	84 ± 60	–	
Platelets (×10^9/l)	240 ± 35	–	

Whether the reduction of Tpo during IGF-I treatment is due to a direct effect of IGF-I on the liver, or whether there exists a negative feedback mechanism between PLT and Tpo synthesis [4], remains to be clarified. The finding that Epo levels do not correlate with the IGF-I induced stimulation of erythropoiesis suggests that this effect is not Epo mediated as was also shown in rats [5] and in children [6]. Recently, it has been suggested that IGF-I secreted by macrophages may directly stimulate erythroblastic islands [7].

ORIT SHEVAH[1]
JOANNE YACOBOVICH[2]
MEIRA ZOLDAN[2]
HANNAH TAMARY[2]
ZVI LARON[1]

[1]Endocrinology and Diabetes Research Unit, Schneider Children's Medical Center, Sackler Faculty of Medicine, Tel-Aviv University, Petah-Tikva, Israel
[2]Division of Oncology Hematology, Schneider Children's Medical Center, Sackler Faculty of Medicine, Tel-Aviv University, Petah-Tikva, Israel
Published online 20 October 2008 in Wiley InterScience (www.interscience.wiley.com).
DOI: 10.1002/ajh.21318
Conflict of interest: Nothing to report.

References

1. Ratajczak J, Zhang Q, Pertusini E, et al. The role of insulin (ONS) and insulin-like growth factor-I (IGF-I) in regulating human erythropoiesis. Studies in vitro under serum-free conditions—Comparison to other cytokines and growth factors. Leukemia 1998;12:371–381.
2. Sivan B, Lilos P, Laron Z. Effects of insulin-like growth factor-I deficiency and replacement therapy on the hematopoietic system in patients with Laron syndrome (primary growth hormone insensitivity). J Pediatr Endocrinol Metab 2003;16:509–520.
3. Merchav S. The haematopoietic effect of growth hormone and insulin-like growth factor I. J Pediatr Endocrinol Metab 1998;11:677–685.
4. Scheding S, Bergmann M, Shimosaka A, et al. Human plasma thrombopoietin levels are regulated by binding to platelet thrombopoietin receptors in vivo. Transfusion 2002;42:321–327.
5. Kling PJ, Taing KM, Dvorak B, et al. Insulin-like growth factor-I stimulates erythropoiesis when administered enterally. Growth Factors 2006;24:218–223.
6. Vihervuori E, Virtanen M, Koistinen H, et al. Hemoglobin level is linked to growth hormone-dependent proteins in short children. Blood 1996;87:2075–2081.
7. Chasis JA, Mohandas N. Erythroblastic islands: Niches for erythropoiesis. Blood 2008;112:470–478.

Int J Hematol
DOI 10.1007/s12185-008-0093-4

ORIGINAL ARTICLE

Pharmacokinetics-based optimal dose-exploration of mycophenolate mofetil in allogeneic hematopoietic stem cell transplantation

Atsuo Okamura · Motohiro Yamamori · Manabu Shimoyama · Yuko Kawano · Hiroki Kawano · Yuriko Kawamori · Shinichiro Nishikawa · Kentaro Minagawa · Kimikazu Yakushijin · Yoshio Katayama · Toshiyuki Sakaeda · Midori Hirai · Toshimitsu Matsui

Received: 15 February 2008 / Revised: 14 March 2008 / Accepted: 4 April 2008

Abstract For better clinical outcomes of mycophenolate mofetil (MMF) in allogeneic hematopoietic stem cell transplantation (alloSCT), higher mycophenolic acid (MPA) plasma levels are proposed to be desirable. Here, we investigate the optimal MMF dosing strategy based on pharmacokinetic studies in 20 Japanese alloSCT patients. The first 11 patients received MMF twice daily at an escalated dose from 15 mg/kg, according to real-time pharmacokinetic monitoring of the total MPA area under the curve (AUC). In the subsequent nine patients, MMF was given at a fixed dose of 1,000 mg three-times daily. The pharmacokinetic data revealed that the dose escalation in each individual did not always increase the AUC. In contrast, the increase of dosing frequency could statistically keep higher MPA plasma levels, as reflected in higher concentration at steady state (C_{ss}) or trough value (C_{trough}). There was no symptomatic adverse event in both groups. These results suggest that MMF administration of every 8 h after alloSCT would be better to maintain higher MPA plasma levels than that of every 12 h even in the same daily dose. Further studies are necessary to confirm the clinical benefit of MMF to prevent graft failure, as well as severe aGVHD.

A. Okamura · M. Shimoyama · Y. Kawano · H. Kawano · Y. Kawamori · S. Nishikawa · K. Minagawa · K. Yakushijin · Y. Katayama · T. Matsui (✉)
Hematology/Oncology, Department of Medicine, Kobe University Graduate School of Medicine, 7-5-1 Kusunoki-cho, Chuo-ku, Kobe 650-0017, Japan
e-mail: matsui@med.kobe-u.ac.jp

M. Yamamori · T. Sakaeda · M. Hirai
Department of Hospital Pharmacy, Kobe University Hospital, 7-5-1 Kusunoki-cho, Chuo-ku, Kobe 650-0017, Japan

Keywords MMF · Pharmacokinetics · Dose escalation · Dosing interval · Engraftment · Acute GVHD

1 Introduction

Both graft failure and severe acute graft-versus-host disease (aGVHD) are potentially fatal complications after allogeneic hematopoietic stem cell transplantation (alloSCT) [1, 2]. The combination of cyclosporine (CSP) or tacrolimus (FK506) with short-course methotrexate (MTX) after alloSCT has been shown to be an effective regimen, and has become the gold standard therapy for prophylaxis against these serious complications [3]. However, toxicities of MTX, such as mucositis in particular, may be severe and debilitating, especially after myeloablative alloSCT. Additionally, MTX may also cause delayed engraftment [4].

Mycophenolate mofetil (MMF) is one of the potent immunosuppressive agents employed as substitute for MTX in alloSCT [4–6]. MMF does not cause severe mucositis and does not pose most of the other potential problems associated with MTX. Moreover, MMF has been reported to facilitate hematopoietic engraftment [6–9].

Mycophenolic acid (MPA), the active metabolite of MMF, interferes with cell proliferation by inhibiting inosine monophosphate dehydrogenase type II, which subsequently blocks de novo purine synthesis in T and B lymphocytes [10].

Pharmacokinetic studies in alloSCT have demonstrated wide inter-individual variations in MPA area under the curve (AUC), as well as in the peak and trough concentrations. In addition, the plasma MPA half-life ranges from 1.5 to 3 h after oral or intravenous administration, which is shorter than that reported in solid organ transplantation [11, 12]. Therefore, the MPA plasma levels in alloSCT are

Brief Communication

Acta Haematologica

Acta Haematol 2008;120:174–176
DOI: 10.1159/000181184

Received: September 29, 2008
Accepted after revision: October 6, 2008
Published online: December 10, 2008

A Marked Increase in Myeloblasts in the Peripheral Blood of a Patient with Burkitt Lymphoma following Granulocyte Colony-Stimulating Factor Administration

Hiroyuki Takamatsu Hirohito Yamazaki Takeshi Yamashita Akiyoshi Takami
Hirokazu Okumura Shinji Nakao

Cellular Transplantation Biology, Kanazawa University Graduate School of Medical Science, Kanazawa, Japan

Granulocyte colony-stimulating factor (G-CSF) mobilizes immature myeloid precursors from the bone marrow of healthy individuals or cancer patients [1–3] as well as abnormal blasts from patients with acute myeloid leukemia (AML) [4, 5]. This report describes a patient with Burkitt lymphoma (BL) who showed a marked increase in normal myeloblasts in the peripheral blood (PB) after G-CSF treatment.

A 43-year-old Japanese male was diagnosed with ileocecal and mediastinal BL. Flow cytometry and fluorescence in situ hybridization analysis demonstrated that the BL cells of the patient had a CD10+, CD19+, CD20+, HLA-DR+ phenotype and the c-MYC/IGH fusion gene. The patient was treated with cyclophosphamide, adriamycin, vincristine and prednisone [6] on 3 March 2007. A rituximab-hyper-cyclophosphamide, vincristine, adriamycin and dexamethasone regimen [7] was started on 20 March. Methotrexate and Ara-C with rituximab [7] were administered on 25 April. G-CSF (filgrastim, 75 μg/day) was administered subcutaneously to accelerate the neutrophil recovery on 29 April and was continued thereafter until 9 May. The leukocyte count started to increase from day 10 of the G-CSF therapy and reached 14.5 × 10^9/l on day 13. At the same time, immature myeloid cells and myeloblasts increased markedly in the PB (fig. 1) from day 12, and this persisted for 8 days after the cessation of G-CSF therapy. The myeloblasts comprised 7% of the peripheral white blood cells at their peak. The surface phenotype of these cells was CD13+, CD33+ and CD34+. The myeloblasts disappeared on day 23 of G-CSF therapy. The BL of this patient was refractory to various chemotherapy regimens and he eventually died of BL 3 months later. During this clinical course, no further increase in myeloblasts in the PB suggestive of AML or MDS was observed.

At first it was difficult to determine whether the myeloblasts were derived from normal or malignant hematopoietic clones because the morphology and surface phenotype of the blasts lacked abnormalities characteristic of leukemic blasts. The rapid decline of the blast cell count after the withdrawal of G-CSF and no signs of either AML or MDS in the patient's subsequent clinical course indicate that the myeloblasts had thus derived from normal hematopoietic stem cells. When G-CSF is given to patients with hematological malignancies after intensive chemotherapy, a slight increase in the number

KARGER

Fax +41 61 306 12 34
E-Mail karger@karger.ch
www.karger.com

0001–5792/08/1203–0174$24.50/0

Accessible online at:
www.karger.com/aha

Hiroyuki Takamatsu, MD, PhD
Cellular Transplantation Biology
Kanazawa University Graduate School of Medical Science
Kanazawa, Ishikawa 920-8641 (Japan)
Tel. +81 76 265 2274, Fax +81 76 234 4252, E-Mail takamaz@med3.m.kanazawa-u.ac.jp

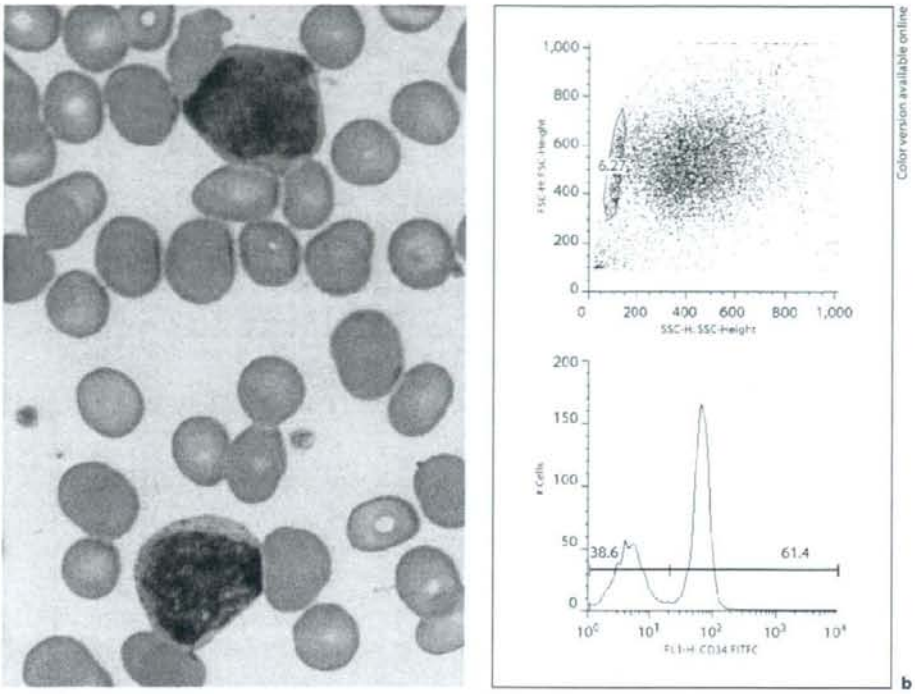

Fig. 1. a Morphology of the PB myeloblasts following G-CSF therapy. **b** Flow cytometric analysis of PB confirmed expression of CD34. The gate was set up for mononuclear cells.

of immature myeloid cells is often seen in the PB. However, a marked increase in immature myeloblasts is rare. Hosokawa et al. [8] reported that a 9-year-old boy with acute lymphoblastic leukemia showed a marked increase in the number of normal myeloblasts in the PB following an intermediate dose of Ara-C (10 × 0.6 g) and G-CSF therapy. Reykdal et al. [9] described a 20-year-old male with T cell lymphoblastic lymphoma showing 30% peripheral normal myeloblasts in PB after treatment with daunorubicin (3 × 60 mg/m^2), Ara-C (0.225 g/m^2) and G-CSF. The myeloblasts in this case were also considered to have originated from normal hematopoietic cells. All 3 patients, including the present case, had lymphocytic leukemia/lymphomas and had been treated with an Ara-C-containing regimen before G-CSF administration. To our knowledge, the present case is the second adult patient who showed a marked increase in the myeloblast count in the PB following G-CSF administration. We could not find any similar reports when we conducted a literature search, including contacts with companies producing G-CSF. It is important to be aware of the fact that normal myeloblasts can appear in the PB of patients with hematologic malignancies after chemotherapy combined with G-CSF, particularly in patients with AML whose leukemic cells lack unique leukemic cell markers.

References

1 Khoury HJ, Loberiza FR Jr, Ringden O, Barrett AJ, Bolwell BJ, Cahn JY, Champlin RE, Gale RP, Hale GA, Urbano-Ispizua A, Martino R, McCarthy PL, Tiberghien P, Verdonck LF, Horowitz MM: Impact of post-transplantation G-CSF on outcomes of allogeneic hematopoietic stem cell transplantation. Blood 2006;107:1712–1716.

2 Teshima T, Sunami K, Bessho A, Shinagawa K, Omoto E, Ueoka H, Harada M, Ohno Y, Miyoshi T, Miyamoto T, Higuchi M: Circulating immature cell counts on the harvest day predict the yields of CD34+ cells collected after granulocyte colony-stimulating factor plus chemotherapy-induced mobilization of peripheral blood stem cell. Blood 1997;89:4660–4661.
3 Boogaerts M, Cavalli F, Cortes-Funes H, Gatell JM, Gianni AM, Khayat D, Levy Y, Link H: Granulocyte growth factors: achieving a consensus. Ann Oncol 1995;6:237–244.
4 Takamatsu H, Nakao S, Ohtake S, Chuhjo T, Yamaguchi M, Shiobara S, Matsuda T: Granulocyte colony-stimulating factor-dependent leukemic cell proliferation in vivo in acute promyelocytic leukemia. Blood 1993; 81:3485–3486.
5 Baer MR, Bernstein SH, Brunetto VL, Heinonen K, Mrozek K, Swann VL, Minderman H, Block AW, Pixley LA, Christiansen NP, Fay JW, Barcos M, Rustum Y, Herzig GP, Bloomfield CD: Biological effects of recombinant human granulocyte colony-stimulating factor in patients with untreated acute myeloid leukemia. Blood 1996;87:1484–1494.
6 Armitage JO, Dick FR, Corder MP, Garneau SC, Platz CE, Slymen DJ: Predicting therapeutic outcome in patients with diffuse histiocytic lymphoma treated with cyclophosphamide, adriamycin, vincristine and prednisone (CHOP). Cancer 1982;50:1695–1702.
7 Thomas DA, Faderl S, O'Brien S, Bueso-Ramos C, Cortes J, Garcia-Manero G, Giles FJ, Verstovsek S, Wierda WG, Pierce SA, Shan J, Brandt M, Hagemeister FB, Keating MJ, Cabanillas F, Kantarjian H: Chemoimmunotherapy with hyper-CVAD plus rituximab for the treatment of adult Burkitt and Burkitt-type lymphoma or acute lymphoblastic leukemia. Cancer 2006;106:1569–1580.
8 Hosokawa T, Tomoda T, Misaki Y, Wakiguchi H, Kurashige T: Marked increase of peripheral blood myeloblasts following G-CSF therapy in a patient with acute lymphoblastic leukemia. Acta Paediatr Jpn 1995;37:78–80.
9 Reykdal S, Sham R, Phatak P, Kouides P: Pseudoleukemia following the use of G-CSF. Am J Hematol 1995;49:258–259.

blood

2008 112: 2160-2162
Prepublished online Jul 2, 2008;
doi:10.1182/blood-2008-02-141325

Expansion of donor-derived hematopoietic stem cells with PIGA mutation associated with late graft failure after allogeneic stem cell transplantation

Kanako Mochizuki, Chiharu Sugimori, Zhirong Qi, Xuzhang Lu, Akiyoshi Takami, Ken Ishiyama, Yukio Kondo, Hirohito Yamazaki, Hirokazu Okumura and Shinji Nakao

Blood (print ISSN 0006-4971, online ISSN 1528-0020), is published semimonthly by the American Society of Hematology, 1900 M St, NW, Suite 200, Washington DC 20036.

Brief report

Expansion of donor-derived hematopoietic stem cells with *PIGA* mutation associated with late graft failure after allogeneic stem cell transplantation

*Kanako Mochizuki,[1] *Chiharu Sugimori,[1] Zhirong Qi,[1] Xuzhang Lu,[1] Akiyoshi Takami,[1] Ken Ishiyama,[1] Yukio Kondo,[1] Hirohito Yamazaki,[1] Hirokazu Okumura,[1] and Shinji Nakao[1]

[1]Cellular Transplantation Biology, Division of Cancer Medicine, Kanazawa University Graduate School of Medical Science, Ishikawa, Japan

A small population of CD55$^-$CD59$^-$ blood cells was detected in a patient who developed donor-type late graft failure after allogeneic stem cell transplantation (SCT) for treatment of aplastic anemia (AA). Chimerism and *PIGA* gene analyses showed the paroxysmal nocturnal hemoglobinuria (PNH)–type granulocytes to be of a donor-derived stem cell with a thymine insertion in *PIGA* exon 2. A sensitive mutation-specific polymerase chain reaction (PCR)–based analysis detected the mutation exclusively in DNA derived from the donor bone marrow (BM) cells. The patient responded to immunosuppressive therapy and achieved transfusion independence. The small population of PNH-type cells was undetectable in any of the 50 SCT recipients showing stable engraftment. The de novo development of donor cell–derived AA with a small population of PNH-type cells in this patient supports the concept that glycosyl phosphatidylinositol–anchored protein–deficient stem cells have a survival advantage in the setting of immune-mediated BM injury. (Blood. 2008;112:2160-2162)

Introduction

Although small populations of CD55$^-$CD59$^-$ blood cells are often detectable in patients with aplastic anemia (AA), it remains unclear how such paroxysmal nocturnal hemoglobinuria (PNH)-type cells arise.[1] We recently encountered a patient with immune-mediated late graft failure (LGF) following allogeneic stem cell transplantation (SCT) for treatment of AA. Analyses of the patient's peripheral blood (PB) and bone marrow (BM) showed hematopoietic stem cells (HSCs) of donor origin with mutant *PIGA*, supporting the concept that glycosyl phosphatidylinositol–anchored protein (GPI-AP)–deficient stem cells have a survival advantage in the setting of immune mediated BM injury.

Methods

Patients

A 59-year-old man underwent allogeneic PBSCT from a human leukocyte antigen (HLA)–matched sibling donor after conditioning with fludarabin (120 mg/m^2), cyclophosphamide (1200 mg/m^2), and antithymocyte globulin (60 mg/kg) for treatment of very severe AA in April 2002 (Table 1) and achieved complete donor chimerism with normal blood cell counts. In January 2006, he developed pancytopenia and was diagnosed as having LGF without residual recipient cells. The patient underwent a second PBSCT from the original donor without preconditioning on February 8, 2006. Pancytopenia resolved completely by day 16 after PBSCT. However, at approximately day 60, the blood counts decreased gradually, and the patient became transfusion-dependent. On day 196 after the second PBSCT, the white blood cell (WBC) count was 5.3×10^9/L with 17% neutrophils, the hemoglobin concentration was 75 g/L, and the platelet count was 22×10^9/L. Treatment with horse antithymocyte globulin (ATG) and cyclosporine was started on day 205 after the second PBSCT. Transfusions were terminated after 88 days of the immunosuppressive therapy. Although the patient presently receives low-dose tacrolimus for treatment of chronic graft-versus-host disease, which developed 1 year after the second PBSCT, his pancytopenia has markedly improved as shown in Table 1. PB and BM of the patient were subjected to analyses of chimerism and flow cytometry to detect CD55$^-$CD59$^-$ cells and *PIGA* gene analysis.

As controls, the PB from 51 SCT recipients (48 with hematologic malignancies and 3 with AA) who achieved a complete recovery of donor-derived hematopoiesis were subjected to flow cytometric analysis for the screening of CD55$^-$CD59$^-$ cells. Of the 51 patients, 4 and 23, respectively, had acute graft-versus-host disease (GVHD) of grade II or higher and chronic GVHD at sampling.

BM aspirates were obtained from the patient's donor and 10 healthy individuals for *PIGA* gene analysis. Informed consent was obtained from all patients and healthy individuals in accordance with the Declaration of Helsinki for blood examination, and the experimental protocol for *PIGA* gene analysis was approved by our participating institutional ethics committee (No.157).

Detection of PNH-type cells

To detect GPI-AP deficient (GPI-AP$^-$), PNH-type cells, we performed high-sensitivity 2-color flow cytometry of granulocytes and red blood cells (RBCs), as described previously.[1] The presence of 0.003% or more CD55$^-$CD59$^-$CD11b$^+$ granulocytes and 0.005% or more CD55$^-$CD59$^-$glycophorin-A$^+$ RBCs was defined as an abnormal increase based on the results in 183 healthy individuals.[2]

Cell sorting and chimerism analysis

CD3$^+$cells were isolated from the PB mononuclear cells of the patient using magnetic-activated cell sorting (MACS) CD3 Microbeads (Miltenyi Biotec, Auburn, CA). The CD55$^-$CD59$^-$CD11b$^+$ granulocytes were separated from the CD55$^+$CD59$^+$CD11b$^+$ granulocytes with a cell sorter (JSAN; Bay Bioscience, Yokohama, Japan). More than 95% of the sorted cells were

Submitted February 21, 2008; accepted June 17, 2008. Prepublished online as *Blood* First Edition paper, July 2, 2008; DOI 10.1182/blood-2008-02-141325.

*K.M. and C.S. contributed equally to this work.

The online version of this article contains a data supplement.

The publication costs of this article were defrayed in part by page charge payment. Therefore, and solely to indicate this fact, this article is hereby marked "advertisement" in accordance with 18 USC section 1734.

Table 1. Hematologic parameters of donor and recipient

	Donor		Recipient			
Date	Apr 2002	May 2008	Before 1st SCT Apr 2002	Before 2nd SCT Jan 2006	At ATG therapy Aug 2006	After 20 mo of ATG therapy Apr 2008
WBC count, $\times 10^9$/L	7.0	5.1	1.2	1.7	5.3	4.0
Neutrophil proportions, %	77	65	0	0	17	62
RBC count, $\times 10^{12}$/L	4.21	4.43	2.20	2.75	2.07	3.04
Reticulocytes, $\times 10^9$/L	not tested	35	2	3	26	61
Hemoglobin, g/L	146	150	72	89	75	120
Platelet count, $\times 10^9$/L	261	230	19	52	22	54

$CD55^-CD59^-CD11b^+$. The *D1S80* locus was amplified from DNA of different cell populations with an AmpliFLP D1S80 PCR Amplification Kit (Perkin-Elmer Cetus, Norwalk, CT).

PIGA gene analysis

The coding regions of *PIGA* were amplified by seminested PCR or nested PCR from DNA extracted from the sorted PNH-type cells using 12 primer sets[3,4] (Table S1, available on the *Blood* website; see the Supplemental Materials link at the top of the online article), and 6 ligation reactions were used to transform competent *Escherichia coli* JM109 cells (Nippon Gene, Tokyo, Japan). Five clones were selected randomly from each group of transfectants and subjected to sequencing with a BigDye Terminator v3.1 Cycle Sequencing Kit (Applied Biosystems, Foster City, CA) and an ABI PRISM 3100 Genetic Analyzer (Applied Biosystems).

Amplification refractory mutation system PCR

On the basis of a mutant sequence detected in *PIGA* of the patient, a nested amplification refractory mutation system (ARMS) forward primer with a 3′-terminal nucleotide sequence complementary to the mutant sequence was prepared[5] (Table S1). To enhance the specificity, a mismatch at the penultimate nucleotide position of the mutation site was incorporated in the ARMS forward primer (P1).[6,7] P1 and a reverse primer (P3) were used to amplify a 127 bp fragment containing the mutant sequence from the exon 2 amplified product. PCR was conducted under the following conditions; denaturation for 30 seconds at 94°C, annealing for 60 seconds at 64°C and extension for 90 seconds at 72°C for 20 cycles. Another forward primer (P2), complementary to the wild-type *PIGA* sequence upstream of the mutation site, was used in combination with P3 to amplify an internal control according to the same condition of ARMS-PCR.

Results and discussion

PNH-type cells were not detected in the donor or the patient at the time of development of the first LGF, whereas 0.147% PNH-type granulocytes and 0.019% PNH-type RBCs were detected in the PB

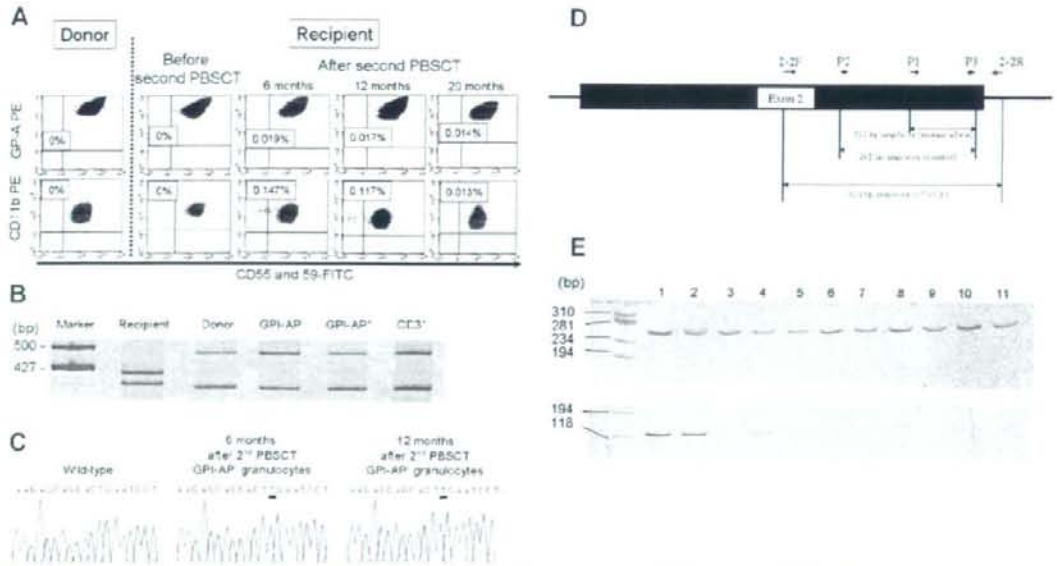

Figure 1. Analysis of PNH-type cells after the second PBSCT. (A) High-sensitivity flow cytometry detected small populations of $CD55^-CD59^-$ cells in both granulocytes and red blood cells at the development of the second LGF as well as in those obtained 6 and 12 months later, but did not detect PNH-type cells in the donor or in the recipient before the second PBSCT. The numbers denote the proportion of PNH-type cells in $CD11b^+$ granulocytes or glycophorin A^+ RBCs. (B) *D1S80* allelic patterns of sorted $GPI\text{-}AP^-$ granulocytes, $GPI\text{-}AP^+$ granulocytes, and $CD3^+$ lymphocytes. The polymerase chain reaction (PCR) products were subjected to 8% polyacrylamide gel electrophoresis and visualized by silver staining. (C) Nucleotide sequences of *PIGA* exon 2 in DNA from PNH-type granulocytes obtained 6 and 12 months after the second PBSCT. (D) A schematic illustration for ARMS-PCR is shown. Primer positions for the first, second are shown by short arrows. A black box and adjacent lines represent exon 2 and introns, respectively. (E) Amplified products of control PCR (the upper gel) and ARMS-PCR (the lower gel) were electrophoresed in 12.5% polyacrylamide gel and visualized by the silver staining. A pMD20-T vector containing the mutated exon 2 fragment was used as a positive control for ARMS-PCR. The template DNA derives from a plasmid containing the mutated exon 2 in lane 1, donor BM in lane 2, donor PB in lane 3, recipient BM in lane 4, recipient PB in lane 5, and BM from healthy individuals in lanes 6 to 11. PCR with a 5′ primer specific to the nucleotide sequence upstream of the mutated sequence amplified a 261 bp fragment from DNA of the donor and all healthy individuals.

obtained at the time of development of the second LGF (Figure 1A). Similar percentages of PNH-type blood cells were detectable in the PB of the patient 6 and 14 months later. When PB from 51 SCT recipients was examined, none of the patients were found to have detectable PNH-type cells (data not shown). PNH-type blood cells were also undetectable in a donor PB sample obtained 21 months later.

The *D1S80* locus allelic pattern of the PNH-type granulocytes in the patient was compatible to that of the donor (Figure 1B). The emergence of donor-derived PNH-type cells and hematologic improvement after immunosuppressive therapy suggest that LGF arises as a result of de novo development of AA which affects the donor-derived hematopoietic stem cells (HSCs).

PIGA gene analysis of the DNA prepared from the sorted PNH-type cells of the patient obtained at the development of LGF and 6 months later showed an insertion of thymine at position 593 (codon 198) in 3 of 5 clones and 5 of 5 clones examined, respectively (Figure 1C). Mutations in other exons were not identified. The presence of a single *PIGA* mutation in PNH-type granulocytes and its persistence over 6 months suggest that these PNH-type cells are derived from a mutant HSC rather than from a committed granulocyte progenitor cell. Moreover, an ARMS-PCR with a 5′ primer specific to the mutated sequence amplified a 127 bp fragment from DNA of the donor BM as well as of the recipient BM and PB while it failed to amplify the same fragment in donor PB and in BM of all 10 healthy individuals (Figure 1D).

These experiments demonstrate that *PIGA*-mutant HSCs were present in the BM of the donor in a dormant state and were transplanted into the recipient and provide, for the first time, in vivo evidence that *PIGA* mutant, GPI-AP–deficient HSCs have a survival advantage in the setting of immune mediated BM injury. Similarly, relative resistance to immune injury likely accounts for the high incidence of PNH observed in association with acquired AA.

Acknowledgments

We thank Ms Shizuka Yasue, Ms Megumi Yoshii, and Ms Rie Oumi for their excellent technical assistance. We also thank Dr Charles Parker for his critical reading of this manuscript.

This work was supported by a Grant-in-Aid for Scientific Research from the Ministry of Education, Culture, Sports, Science and Technology of Japan (No.15390298), a grant from the Ministry of Health, Labour and Welfare of Japan, and a grant from the Japan Intractable Diseases Research Foundation.

Authorship

Contribution: K.M. and C.S. participated in designing and performing the research. Z.Q. and X.L. performed experiments. K.M., C.S., and S.N. wrote the paper. C.S., A.T., K.I., Y.K., H.Y., and H.O. provided patient care. All authors have approved the final version of the manuscript.

Conflict-of-interest disclosure: The authors declare no competing financial interests.

Correspondence: Shinji Nakao, Cellular Transplantation Biology, Division of Cancer Medicine, Kanazawa University Graduate School of Medical Science, 13-1 Takaramachi, Kanazawa, Ishikawa 920-8641, Japan; e-mail: snakao@med3.m.kanazawa-u.ac.jp.

References

1. Sugimori C, Chuhjo T, Feng X, et al. Minor population of CD55-CD59- blood cells predicts response to immunosuppressive therapy and prognosis in patients with aplastic anemia. Blood. 2006;107:1308-1314.
2. Sugimori C, Yamazaki H, Feng X, et al. Roles of DRB1 *1501 and DRB1 *1502 in the pathogenesis of aplastic anemia. Exp Hematol. 2007;35:13-20.
3. Kai T, Shichishima T, Noji H, et al. Phenotypes and phosphatidylinositol glycan-class A gene abnormalities during cell differentiation and maturation from precursor cells to mature granulocytes in patients with paroxysmal nocturnal hemoglobinuria. Blood. 2002;100:3812-3818.
4. Mortazavi Y, Merk B, McIntosh J, et al. The spectrum of PIG-A gene mutations in aplastic anemia/paroxysmal nocturnal hemoglobinuria (AA/PNH): a high incidence of multiple mutations and evidence of a mutational hot spot. Blood. 2003;101:2833-2841.
5. Newton CR, Graham A, Heptinstall LE, et al. Analysis of any point mutation in DNA. The amplification refractory mutation system (ARMS). Nucleic Acids Res. 1989;17:2503-2516.
6. Dang RK, Anthony RS, Craig JI, Leonard RC, Parker AC. Limitations of the use of single base changes in the p53 gene to detect minimal residual disease of breast cancer. Mol Pathol. 2002;55:177-181.
7. Bai RK, Wong LJ. Detection and quantification of heteroplasmic mutant mitochondrial DNA by real-time amplification refractory mutation system quantitative PCR analysis: a single-step approach. Clin Chem. 2004;50:996-1001.

Thrombosis Research (2008) 123, 274–280

ELSEVIER

THROMBOSIS RESEARCH

www.elsevier.com/locate/thromres

REGULAR ARTICLE

Expression of annexin II in human atherosclerotic abdominal aortic aneurysms

Tomoe Hayashi [a,*], Eriko Morishita [a], Hiroshi Ohtake [b], Yoshio Oda [c], Kazuhide Ohta [d], Masahisa Arahata [a], Yasuko Kadohira [a], Mio Maekawa [a], Yasuo Ontachi [a], Masahide Yamazaki [a], Hidesaku Asakura [a], Akiyoshi Takami [a], Shinji Nakao [a]

[a] *Cellular Transplantation Biology, Kanazawa University Graduate School of Medicine, 13-1, Takaramachi, Kanazawa, 920-8641, Japan*
[b] *Department of General and Cardiothoracic Surgery, Kanazawa University Graduate School of Medicine, Kanazawa, Japan*
[c] *ALP Pathological Institute, Kanazawa, Japan*
[d] *Department of Pediatrics, Kanazawa University Graduate School of Medicine, Kanazawa, Japan*

Received 10 October 2007; received in revised form 4 February 2008; accepted 23 March 2008
Available online 27 May 2008

KEYWORDS
Annexin II;
Abdominal aortic aneurysm;
Atherosclerosis

Abstract

Background: Annexin II is a receptor for tissue-type plasminogen activator (t-PA) that converts plasminogen to plasmin. Although the fibrinolytic system is known to play an important role in the pathogenesis of abdominal aortic aneurysms (AAAs), the relationship between annexin II and AAA development is unknown. Therefore, we examined annexin II localization in the wall of human atherosclerotic AAAs.
Methods and Results: Specimens from 13 patients undergoing elective repair of an AAA were taken. Annexin II expression was evaluated by immunohistochemical analysis. Immunostaining results were semiquantitatively analyzed using histology scores and WinROOF software based on staining intensity. The expression of annexin II was increased and the histology score was higher in the shoulder region of the atheromatous plaque than in the atheroma and fibrous plaque regions. Annexin II appeared to have greater expression and the histology score was higher in regions where the media was preserved. Furthermore, there was a significant inverse correlation between AAA size and histology score in the fibrous plaque region.
Conclusions: The present work demonstrates various levels of annexin II expression within the aneurysm wall. Therefore, we suggest that alteration of annexin II

* Corresponding author. Tel.: +81 76 265 2275; fax: +81 76 234 4252.
E-mail address: tomoeha@aol.com (T. Hayashi).

doi:10.1016/j.thromres.2008.03.027

expression within the aortic wall may be associated with the development of an aneurysm.

Introduction

Abdominal aortic aneurysm (AAA) is a common and highly lethal disease. The destruction of elastin is considered to be one of the major factors responsible for the pathogenesis of AAA. As elastic fibers normally maintain the structure of the vascular wall against hemodynamic stress, proteolytic degradation induces disorganized extracellular remodeling, leading to progressive aortic enlargement and ultimate rupture [1].

The fibrinolytic system also plays an important role in the process of extracellular-matrix (ECM) remodeling [2], and there have been many reports on its expression in the vessel wall [3,4]. In this system, two plasminogen activators (PAs), tissue-type (t-PA) and urokinase-type (u-PA), generate plasmin from the inactive proenzyme plasminogen. Plasmin is a trypsin-like proteolytic enzyme capable of directly degrading some components of the ECM, as well as activating matrix metalloproteinases (MMPs) [5]. MMPs are known to degrade the ECM, including collagen and elastin, impairing the structural integrity of the vascular wall [6–8]. Previous studies demonstrated increased fibrinolytic activity and t-PA and u-PA gene expression in atherosclerotic human aortic aneurysms compared with nondilated atherosclerotic aortic wall and normal aorta [9,10]. In addition, other reports showed that t-PA and u-PA mRNA as well as their immunoreactivities were increased within the aneurysmal wall [11]. These data suggest that the fibrinolytic balance in the aneurysmal wall is disturbed, and this imbalance may lead to increased plasmin generation, activation of MMPs, and structural degeneration of the vessel wall.

Annexin II has been described as a receptor for fibrinolytic proteins and belongs to a family of calcium-regulated, phospholipid-binding, membrane proteins [12,13]. Annexin II is mainly expressed on the surface of vascular endothelial cells and is also found in some epithelial cells [13,14], promyelocytic leukemia cells [15], and cells of several monocyte-like lines [16]. According to kinetic studies, annexin II binds plasminogen and t-PA independently, thereby enhancing the catalytic efficiency of plasminogen activation by 60-fold [13]. As annexin II has a variety of biological activities, it was recently shown that annexin II plays an important role in the pathophysiological action of macrophages during the inflammatory process, and facilitates plasminogen-mediated matrix invasion and degradation by macrophages [17].

In this study, we used immunohistochemical analysis to detect the expression of annexin II in atherosclerotic AAAs. In addition to identifying specific areas of annexin II expression, we also described various levels of annexin II expression according to the magnitude of destruction of elastic fibers in the tunica media. These results suggest a linkage between atherosclerosis, enhanced fibrinolysis, and the potential breakdown of the vessel wall.

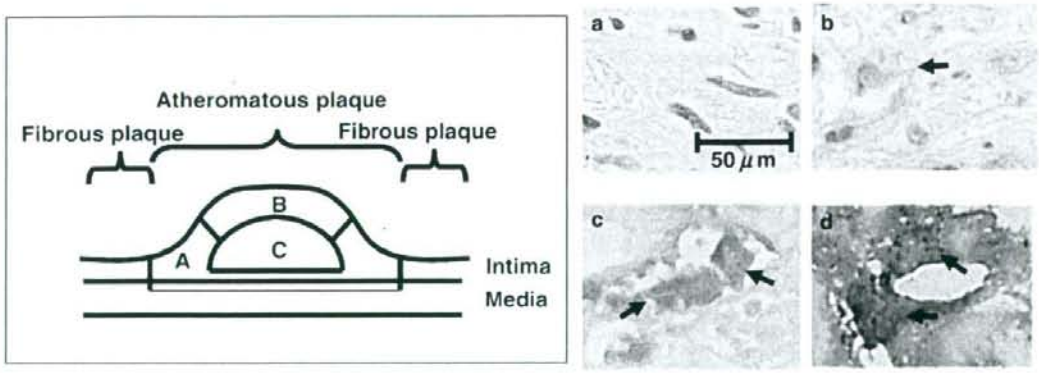

Figure 1 Schematic showing a portion of the atheromatous plaque, as described in Materials and Methods. (A): shoulder region, (B): fibrous cap, (C): atheroma. Histological classification of the cells according to their immunointensity. Representative immunohistochemical images for Annexin II (red stain) are shown in each panel. a: 0, negative, b: 1+, weekly positive, c: 2+, moderately positive, d: 3+, strongly positive.

Material and Methods

Sample collection

All procedures were approved by the local scientific ethical committee and reported to the data protection authorities. Specimens of vascular tissue were obtained with informed consent from 13 consecutive patients (11 males, 2 females, mean age: 73.1 years, ranging from 63 to 83 years) with an atherosclerotic risk profile (hypertension, 92%; dyslipidemia, 54%; smoking, 46%) undergoing elective resection of an AAA at the Kanazawa University Graduate School of Medicine. The mean size of the aneurysm, measured as maximal infrarenal aortic transverse diameter by ultrasound or CT, was 5.9 ± 1.2 cm (range, 4.0 to 7.7 cm). None of the patients suffered from AAA rupture at the time of surgery. Specimens were taken from the anterior wall of the part of the aneurysm with the largest diameter. Specimens were immediately fixed in 10% formalin at room temperature for 24 hr, embedded in paraffin, and cut into sections.

Light microscopy

Each paraffin section was stained with hematoxilin-eosin (H & E) and elastica van Gieson. For analysis, we used light microscopy to examine aortic tissues divided into the regions of the fibrous plaque (free of atheroma) and the atheromatous plaque. Moreover, the atheromatous plaque was subdivided into shoulder, fibrous cap, and atheroma (lipid core) regions (Fig. 1A, B and C).

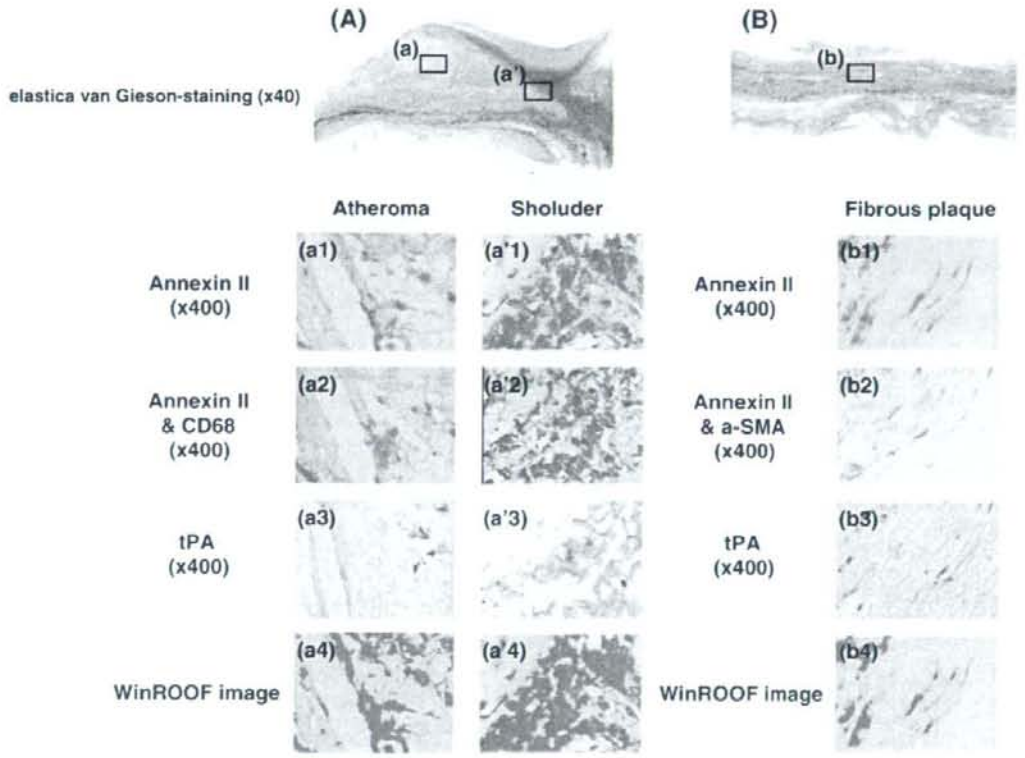

Figure 2 Immunohistochemical localization of annexin II in the human AAA wall. Atherosclerotic vessel wall specimens from AAAs were analyzed by elastica van Gieson (EVG) staining, tPA immunostaining, and double-immunostaining for CD68 and annexin II, or α-smooth muscle actin (α-SMA) and annexin II. (A) Atheromatous plaque region. There were marked inflammatory infiltrates in the shoulder region (a'). Annexin II expression (red stain) in atheroma and the shoulder region are shown in a1 and a'1, respectively. Annexin II expression in the atheroma and shoulder region mainly colocalized with CD68+ macrophage (brown stain) in the atheroma (a2) and shoulder (a'2) region of the atheromatous plaque. (B) Fibrous plaque region. Annexin II expression (red stain) in the fibrous plaque region is shown in b1. Annexin II expression in the fibrous plaque region is mainly colocalized withα-SMA-positive cells (brown stain) shown in b2. tPA expression (brown stain) was observed in parallel with expression of annexin II (a3, a'3, and b3). The corresponding digitized images analyzed with WinROOF software are shown in a4, a'4, and b4, respectively. The annexin II-positive areas are displayed in green.

Immunohistochemistry

Immunohistochemical staining for annexin II (sc-9061, diluted 1:100, Santa Cruz Biotechnology, Inc., CA, USA) and tPA (goat anti-human tPA antibody, No.387, American Diagnostica Inc., CT, USA) was performed with the use of the EnVision+System (DakoCytomation Denmark A/S, Glostrup, Denmark). Furthermore, in order to identify which type of cells contained annexin II in the artery walls, α-smooth muscle actin (α-SMA) and annexin II, or CD68 and annexin II were double-immunostained in the same tissue sections. Formalin-fixed, paraffin-embedded tissue sections were routinely deparaffinized. For antigen retrieval, the tissue slides were treated with trypsin (Histofine trypsin solution, Nichirei, Tokyo, Japan) for α-SMA, or pepsin (Histofine pepsin solution, Nichirei) for CD68. Endogenous peroxidase activity and nonspecific antigen sites were blocked with 1% hydrogen peroxide solution for 5 min, and 4% goat serum for 15 min at room temperature. The sections were then incubated overnight at 4 °C with mouse monoclonal anti-human α-SMA antibody (clone asm-1, diluted 1:50, Novocastra, Newcastle, UK) or mouse monoclonal anti-human CD68 antibody (clone KP-1, diluted 1:100, DakoCytomation Denmark A/S, Glostrup, Denmark), followed by application of the EnVision+System using the peroxidase method (brown stain). After the coloring reaction, the tissue sections were washed in distilled water and microwaved in 10 mM citrate buffer (pH 6.0) for 5 min for annexin II antigen retrieval. They were then incubated overnight at 4 °C with rabbit polyclonal anti-human annexin II antibody, followed by application of the EnVision-AP System (DakoCytomation Denmark A/S) using the alkaline phosphatase method (red stain). The tissue slides were counterstained with Mayer's hematoxylin and mounted.

Histology score-based semiquantitative analysis

Semiquantitative analysis using histology-scores was based on previously-described methods [18,19]. Briefly, the immunointensity of the cells was assessed in five randomly selected 200 μm square areas in each region, under microscopic observation at ×200 magnification, and then graded as follows: 0, negative; 1+, weakly positive; 2+, moderately positive; and 3+, strongly positive (Fig. 1. a-d). The histology score was based on the number of positive cells (Pi) and their staining intensity (i), and was calculated in each region according to the following formula: Histology Score = $\Sigma(i \times Pi)$, i = 1,2, or 3, and Pi varies.

Computer-assisted semiquantitative analysis

To confirm the results of the histology-score method objectively, we performed computer-assisted analysis using WinROOF image-processing software (Mitani Corp., Tokyo, Japan). This software allowed accurate identification and calculation of the immunostained area. The macroinstruction was composed of algorithms for color identification based on red-green-blue (RGB) and hue-luminosity-saturation (HLS) parameters. We set the macroinstruction, which extracted almost all grades of intensity ranging from weak to strong, and then calculated the ratio of the immunostained area to the corresponding area evaluated by the histology-score method (i.e., the area which was cut from the extracted images at a size of 200 μm square in each part) (Fig. 2. a4, a'4, and b4).

Statistical analysis

All data are shown as the mean±standard error (se), and coefficient of variation (CV). Statistical analysis was performed with a Wilcoxon signed-rank test and analysis of variance (Non-Parametric ANOVA), followed by Scheffé's post hoc test. A correlation analysis was performed using Spearman's rank correlation test. Statistical significance was established at the $p<.05$ level.

Results

Copious extracellular matrix components and inflammatory infiltrates were found in the intima, especially in the shoulder

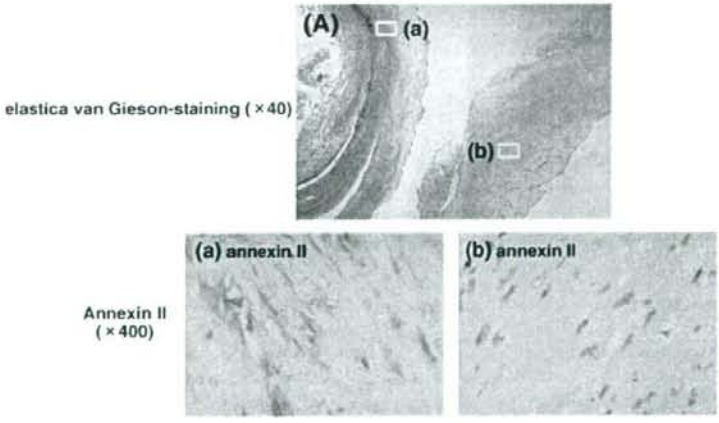

Figure 3 A: Representative histological sections stained with elastica van Gieson (×40), which showed a good contrast between elastin (black), collagen (pink), and smooth muscle cells (yellow). (a) (b): Immunohistochemical demonstration of annexin II expression in the area with preserved tunica media (a) and without media (b). The annexin II expression appeared to be higher in regions with preserved media.

region of the atheromatous plaque, and elastic fibers were fragmented in parts, as shown by elastica van Gieson's staining (Fig. 2A and B).

Localization of Annexin II protein in the aneurysmal wall

Annexin II expression in the aneurysmal wall was analyzed by immunohistochemistry. The expression of annexin II was substantially increased in the shoulder region of the atheromatous plaque (Fig. 2. a'1), as compared with the atheroma and the fibrous plaque regions (Fig. 2. a1 and b1). As shown in Fig. 4A, the histology score was significantly higher ($p<0.01$) in the shoulder region (427±282, 0.66) than in the atheroma (54.0±34.6, 0.64) and the fibrous plaque regions (130±53.2, 0.41). The fibrous cap region was preserved in some specimens, and the expression of annexin II was substantially increased in this region. However, we could not obtain five 200 μm square areas for determination of the histological score, as they were peeled away in the process of taking specimens.

The expression of annexin II in the shoulder region was mainly colocalized with CD68-positive macrophages (Fig. 2. a'2), and α-SMA-positive smooth muscle cells also expressed annexin II in the fibrous plaque region (Fig. 2. b2). Moreover, Annexin II expression was confirmed by the consistent expression of tPA (Fig. 2. a3, a'3 and b3). As expected, the intimal endothelium of the aneurysmal wall and the endothelial cells of capillaries within the wall also expressed annexin II. Annexin II was expressed ubiquitously in the adventitia of every specimen.

To determine the relationship between elastic fibers and annexin II expression, we selected eight cases in which there was a distinct line of demarcation of preservation of elastic fibers in the media and compared the expression of annexin II in the intima with or without elastic fibers. The annexin II expression appeared to be higher in regions where the elastic fibers were preserved (Fig. 3. (a), (b)). The histology score

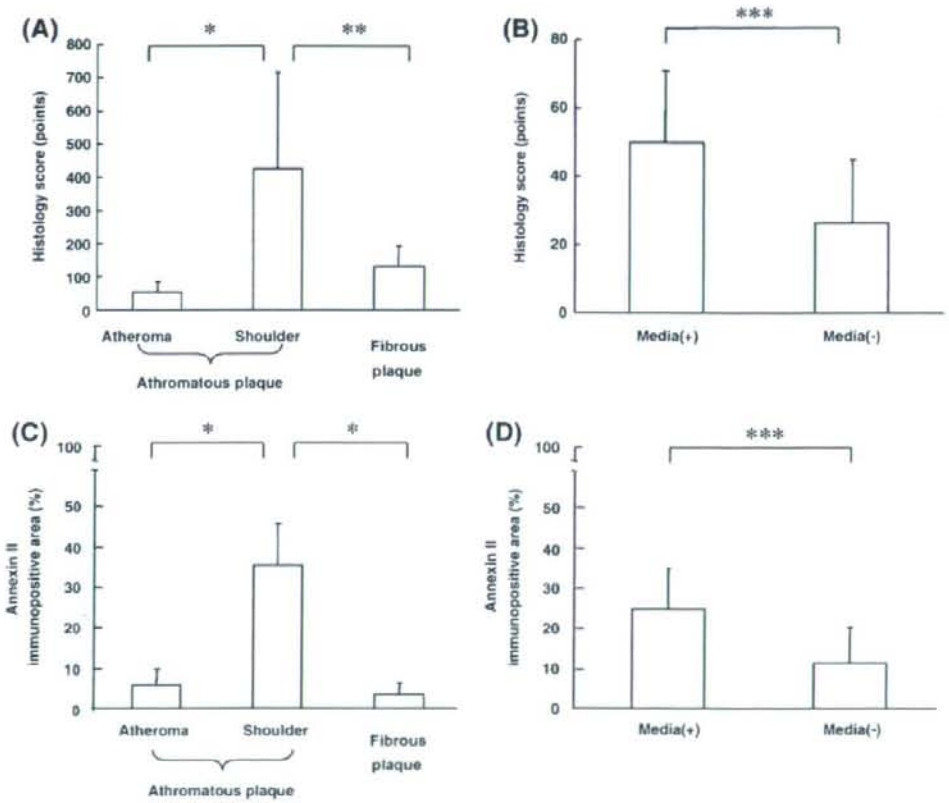

Figure 4 Histology score and the ratio of the annexin II immunopositive area to the histology score in each region (calculated by WinROOF). A: Histology score in the atheroma and shoulder regions of the atheromatous plaque and fibrous plaque region. B: Histology score in the area with and without preserved tunica media. C: The ratio of the immunopositive area in the atheroma and shoulder regions of the atheromatous plaque and fibrous plaque region. D; The ratio of the immunopositive area in regions with and without preserved tunica media. Each bar represents $x \pm SD$. *$p<0.0001$, **$p<0.001$, *** $p<0.05$.

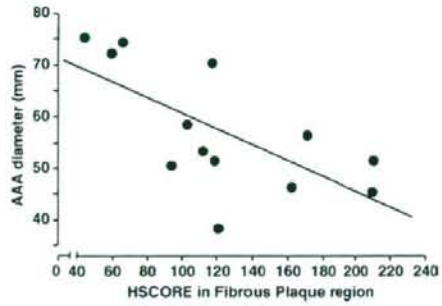

Figure 5 Relationship between the AAA diameter and the histology score (HSCORE) in the fibrous plaque region. There was a significant inverse correlation (Spearman's rank test) between the AAA diameter and the histology score ($r^2 = 0.441$, $p < 0.05$).

was also higher in the area with elastic fibers (49.9±21.5, 0.43) than without elastic fibers (26.4±20.0, 0.76), and the difference was statistically significant ($p < 0.05$; Fig. 4B). There was no significant difference between regions in the number of infiltrated cells.

To compensate for a lack of objectivity of the histology-score method, a computer-assisted semiquantitative analysis was also performed using WinROOF software. The ratio of the immunopositive area was significantly higher ($p < 0.0001$) in the shoulder region (35.5±10.4%, 0.29) than in the atheroma (5.72±4.22%, 0.74) and the fibrous plaque regions (3.39±2.52%, 0.74) (Fig. 4C). When we analyzed the results based on the presence of elastic fibers, the ratio of the immunopositive area was significantly higher ($p < 0.05$) in the area with elastic fibers (24.4±12.0%, 0.49) than without elastic fibers (11.1±9.11%, 0.82) (Fig. 4D).

There was a weak but significant correlation between the histology score and the ratio of the immunopositive area based on the WinROOF analysis ($r^2 = 0.264$, $p < 0.01$).

Correlation between AAA size and annexin II expression

To clarify the role of annexin II in AAA formation, it is extremely important to understand the magnitude of annexin II expression in AAAs of different size. We therefore examined the correlation between the AAA size and the histology score or the ratio of the immunopositive area calculated by WinROOF. As shown in Fig. 5, there was a weak but significant inverse correlation between the AAA size and histology score in the fibrous plaque region ($r^2 = 0.441$, $p < 0.05$). Furthermore, there was also an inverse, nonsignificant correlation between the AAA diameter and both the histology score and the ratio of the immunopositive area in the shoulder region.

Discussion

Advanced, complicated atherosclerotic lesions tend to have a fibrous cap that covers a necrotic core and expands at the shoulder region. Macrophages enter, accumulate, and are activated at the shoulder region; this is where apoptosis may occur. In this study, we showed numerous inflammatory cells infiltrating the shoulder region of the atheromatous plaque, and a high histology score for annexin II colocalized with CD68-positive macrophages in this area. This is the first report that showed the annexin II expression in the human atherosclerotic aneurysmal vessel wall. These results suggest that there may be a relationship between the expression of annexin II and the progression of atherosclerosis in the aneurysmal wall.

Several studies point to a significant role of t-PA in atherogenesis, although less is known about the role of t-PA than u-PA. Stein et al. reported that t-PA was produced by macrophages in the arterial wall in severe atherosclerosis [20] and Schneiderman et al. showed similar results in AAAs [10]. In addition, it has been reported that t-PA-induced plasmin generation and monocyte migration are partially dependent on annexin II, and macrophage secretion of t-PA and its annexin II-mediated activation of plasminogen at the cell surface could play an important role in matrix remodeling [17]. A recent report also indicated that annexin II-mediated plasmin production triggers macrophage cytokine expression in atherosclerotic lesions [21], suggesting that annexin II is closely involved in the progression of intimal legions in aortic aneurysms as well as other atherosclerotic diseases.

In addition to the annexin II expression by intimal monocytes/macrophages, we also confirmed annexin II expression by smooth muscle cells in the tunica media of the aortic aneurysm wall. Annexin II expression was enhanced in lesions with residual elastic fibers, or in small-sized lesions. These findings suggest that annexin II expression might be enhanced in lesions in the earlier stage of aneurysm formation.

Regarding the cause of aortic aneurysms, it has been considered that plasmin expression degrades elastic fibers via activation of MMP, resulting in destruction of the wall structure [6–8]. Our result suggest that annexin II-dependent plasmin production in the early stage of aneurysm formation may indirectly degrade elastic fibers via activation of MMP, and this effect diminishes as the aneurysm expands. However, based on our study alone, it is unclear whether enhanced annexin II expression is actually involved in aneurysm formation. It is possible that a change in annexin II dynamics is not the cause but rather the result of aneurysm formation. It is also unclear whether annexin II expression is really decreased in advanced lesions, and the mechanism involved in a shift from enhanced to decreased expression is unknown. There may be a mechanism in